Pincher-generated Nogo-A endosomes mediate growth cone collapse and retrograde signaling

Armela Joset,[1] Dana A. Dodd,[2] Simon Halegoua,[3] and Martin E. Schwab[1]

[1]Brain Research Institute, University of Zurich, and Department of Biology, Eidgenössische Technische Hochschule Zurich, 8057 Zurich, Switzerland
[2]Department of Microbiology, University of Texas Southwestern Medical Center, Dallas, TX 75390
[3]Department of Neurobiology and Behavior, Stony Brook University, Stony Brook, NY 11794

Nogo-A is one of the most potent myelin-associated inhibitors for axonal growth, regeneration, and plasticity in the adult central nervous system. The Nogo-A–specific fragment NogoΔ20 induces growth cone collapse, and inhibits neurite outgrowth and cell spreading by activating RhoA. Here, we show that NogoΔ20 is internalized into neuronal cells by a Pincher- and rac-dependent, but clathrin- and dynamin-independent, mechanism. Pincher-mediated macroendocytosis results in the formation of NogoΔ20-containing signalosomes that direct RhoA activation and growth cone collapse. In compartmentalized chamber cultures, NogoΔ20 is endocytosed into neurites and retrogradely transported to the cell bodies of dorsal root ganglion neurons, triggering RhoA activation en route and decreasing phosphorylated cAMP response element binding levels in cell bodies. Thus, Pincher-dependent macroendocytosis leads to the formation of Nogo-A signaling endosomes, which act both within growth cones and after retrograde transport in the cell body to negatively regulate the neuronal growth program.

Introduction

One of the most potent neurite growth inhibitors of the adult central nervous system (CNS) is the transmembrane protein Nogo-A (Schwab, 2004; Cafferty and Strittmatter, 2006; Yiu and He, 2006). The suppression of Nogo-A signaling by either Nogo-A neutralization, a blockade of the Nogo66 receptor (NgR), or inhibition of downstream signaling components such as RhoA and RhoA kinase (ROCK) leads to enhanced regeneration and nerve fiber growth associated with increased functional recovery in the adult CNS after injury (Schwab, 2004; Cafferty and Strittmatter, 2006; Yiu and He, 2006). Besides its role in the injured mammalian CNS, Nogo-A acts as a regulator of neuronal growth and plasticity in the intact CNS. For instance, the plasticity of the visual cortex is extended beyond the normal postnatal critical period in mice lacking NgR or Nogo-A/B (McGee et al., 2005). In the intact adult spinal cord and cortex, genetic ablation of Nogo-A resulted in an enhanced expression of many proteins involved in neuronal growth and

cytoskeletal organization in the neurons and growth cones (Montani et al., 2009).

Nogo-A is a large membrane protein of 1,163 amino acids containing two main inhibitory regions for neurite growth (GrandPré et al., 2000; Prinjha et al., 2000; Oertle et al., 2003). The 66–amino acid region in the C-terminal domain (Nogo66), also common to other Nogo splice variants, i.e., Nogo B and C, binds to the Nogo66 receptor NgR (Fournier et al., 2001; Barton et al., 2003; He et al., 2003). The Nogo66 signaling complex involves NgR, p75/Troy, LINGO-1, and, at least in some types of neurons, PirB (Fournier et al., 2001; Wong et al., 2002; Mi et al., 2004; Atwal et al., 2008). This signaling complex can also be activated by other myelin inhibitory proteins like myelin-associated glycoprotein (MAG) and oligodendrocyte myelin glycoprotein (OMgp; David and Lacroix, 2003; Filbin, 2003; Yiu and He, 2003). However, blocking NgR does not completely abolish myelin inhibition of neurite outgrowth, which suggests the existence of an NgR-independent mechanism (Kim et al., 2004). A 181–amino acid region in the central region of

The Rockefeller University Press $30.00
J. Cell Biol. Vol. 188 No. 2 271–285
www.jcb.org/cgi/doi/10.1083/jcb.200906089

JCB **271**

THE JOURNAL OF CELL BIOLOGY

the Nogo-A protein called NogoΔ20 is Nogo-A specific and is highly inhibitory for spreading and outgrowth of neurons and fibroblast even in the absence of NgR (Oertle et al., 2003). The in vivo application of the monoclonal antibody 11C7, which is directed against this region and blocks NogoΔ20 function, leads to enhanced regrowth and regenerative sprouting of spinal axons after spinal cord lesion in rats and monkeys (Liebscher et al., 2005; Freund et al., 2006, 2009). In vitro, NogoΔ20 induces growth cone collapse and activates the small GTPase RhoA (Niederöst et al., 2002; Fournier et al., 2003; Oertle et al., 2003). However, the molecular mechanisms underlying NogoΔ20 signaling remain mostly unknown.

Similar to the neutrophic factors, including NGF, brain-derived neutrophic factor (BDNF), and neutrophin 3 or 4 (NT-3 and NT-4; Huang and Reichardt, 2001; Campenot and MacInnis, 2004; Wu et al., 2009), Nogo-A acts locally, at the growth cone. In addition, the members of the neutrophin family induce changes in gene transcription in the cell body upon retrograde axonal transport (Ginty and Segal, 2002; Howe and Mobley, 2005). Detailed analysis of NGF retrograde signaling led to the characterization of a so called NGF "signalosome," a signaling endosome containing endocytosed ligand–receptor complexes and downstream effectors (Ginty and Segal, 2002; Campenot and MacInnis, 2004; Howe and Mobley, 2005). Up to now, the possible role of endocytic signaling as a mechanism for Nogo-A action, both locally and at the level of cell body, has not been investigated.

Here, we show that NogoΔ20 actions on growth cone collapse require signaling from endosomes that contain activated Rho. Internalization of NogoΔ20 into the signaling endosomes is clathrin independent and occurs by Pincher-dependent endocytosis. The subsequent retrograde axonal transport of NogoΔ20 in dorsal root ganglion (DRG) neurons results in increased Rho-GTP and decreased levels of phosphorylated cAMP response element binding (pCREB) in the soma.

Results

The Nogo-A active fragment NogoΔ20 is rapidly internalized into neurons

To examine whether the Nogo-A active fragment NogoΔ20 is internalized into Nogo-A–responsive cells, PC12 neuron-like cells were incubated with 300 nM T7-tagged NogoΔ20 fragment (Oertle et al., 2003). As control, we used 300 nM NogoΔ21-T7, a Nogo-A fragment without inhibitory activity at this concentration (Oertle et al., 2003). First, we incubated PC12 cells with Nogo fragments for 1 h at 4°C, a temperature that prevents endocytosis and vesicular trafficking. PC12 cells immunostained for the T7 tag and analyzed by confocal microscopy displayed patchy staining at the cell surface (Fig. 1 A). When the PC12 cells were incubated with the NogoΔ20 fragment for 15 (Fig. 1 B) or 30 min (Fig. 1 C) at 37°C, the tagged protein was massively endocytosed in small cytosolic vesicles. The control fragment NogoΔ21-T7 could not be detected, either on the cell surface or intracellularly after incubation of PC12 cells (unpublished data). The early endosomal antigen EEA-1, a marker of the early endosome (Mu et al., 1995), colocalized with 40.57 ± 2.65% (n = 47 cells) of NogoΔ20-T7–positive

vesicles after 15 min (Fig. 1, B and E) and with 57.87 ± 3.99% (n = 42 cells) after 30 min (Fig. 1, C and E). The internalization of NogoΔ20 was further characterized by subcellular fractionation. PC12 cells were incubated with 300 nM NogoΔ20 for 30 min at 37°C, lysed, and subjected to a 8–40.6% sucrose step gradient centrifugation. NogoΔ20 was detected in the fractions with lower sucrose concentration, F1 (8–25%) and F2 (25–35%), which contained early endosomes as indicated by EEA-1 (Fig. 1 D). In contrast, NogoΔ20 was absent from the nuclear fraction (containing nucleoporin p62 and from fraction F3 containing mostly endoplasmic reticulum and Golgi membranes (high sucrose concentration of 35–40.6%; Fig. 1 F).

The fate of the growth inhibitory Nogo-A fragment NogoΔ20 was also studied in hippocampal neurons dissected from embryonic day 19 (E19) rats, cultured for 4 d. Incubation with 300 nM NogoΔ20-T7 for 30 min at 37°C resulted in many small fluorescent vesicles spread throughout the cytoplasm of cell bodies and neurites; many of these vesicles (51.45 ± 3.64%) were positive for the early endosomal marker EEA-1 (Fig. 1, D and F). These findings show that upon surface binding, Nogo-Δ20 is rapidly internalized into neuronal endosomes.

To investigate a possible contribution of the Nogo66 receptor subunit NgR to the NogoΔ20 internalization, PC12 cells were treated with phosphatidylinositol-specific phospholipase C (PI-PLC) to remove glycosyl phosphatidylinositol–anchored proteins including NgR from the cell surface (Fournier et al., 2001), or, alternatively, with the peptide NEP1-40, an NgR antagonist (GrandPré et al., 2002). Neither PI-PLC (Fig. S1, A and D) nor NEP1-40 (Fig. S1, B and D) treatment affected NogoΔ20 internalization. In addition, we also observed NogoΔ20 internalization into 3T3 cells, a cell line that does not express NgR (Fig. S1, C and D; Fournier et al., 2001; Oertle et al., 2003). These data demonstrate that NogoΔ20 internalization is not dependent on the Nogo66 receptor NgR.

NogoΔ20 internalization does not follow the conventional endocytic routes

To test whether NogoΔ20-T7 is internalized via one of the classical endocytic routes mediated by clathrin, caveolin, or cholesterol, pharmacological inhibitors and dominant-negative (dn) constructs were used (Fig. 2 A).

Eps15 is crucial for clathrin-coated pit assembly; overexpression of dn Eps15 blocks clathrin-dependent internalization (Benmerah et al., 1998). Transfection of PC12 cells with the dn Eps15 EΔ95/295 did not inhibit internalization of NogoΔ20-T7 (94.58 ± 5.84 vs. 99.93 ± 7.61 in control, n = 294 vs. 323 cells; Fig. 2, B and E). In contrast to NogoΔ20, internalization of transferrin, a well-established marker for clathrin-mediated uptake (Dautry-Varsat et al., 1983; Hopkins, 1983), was dramatically reduced (9.44% ± 2.33 vs. 99.88 ± 5.75% in control, n = 279 vs. 216 cells; ***, P < 0.001; Fig. 2, B and E). These results show that Eps15-mediated clathrin assembly is not essential for NogoΔ20-T7 endocytosis.

The small GTPase dynamin II is involved in the formation of both clathrin-coated and caveolar vesicles (De Camilli et al., 1995; Oh et al., 1998; Pelkmans et al., 2002). Surprisingly, the expression of a dn dynamin II mutant, dynaminK44A
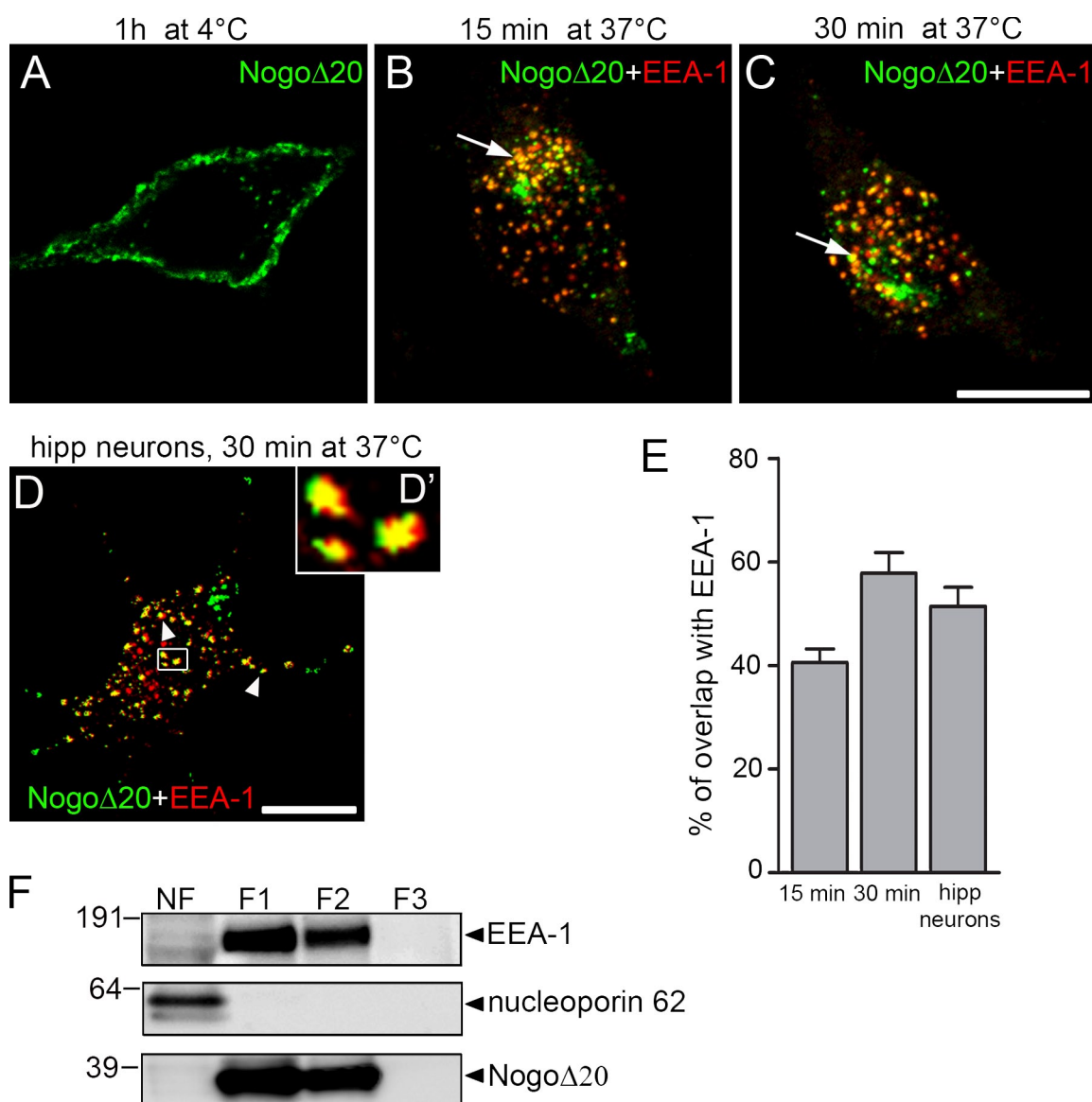
Figure 1. **Surface binding and internalization of NogoΔ20 in neuronal cells.** (A–C) Representative confocal immunofluorescence optical sections of PC12 cells that were incubated with 300 nM NogoΔ20-T7 for 1 h at 4°C (A), or for 15 min (B) or 30 min (C) at 37°C. Cells were stained with anti-T7 mAb for NogoΔ20 (green) and with anti–EEA-1 as an early endosomal marker (red), and analyzed by confocal microscopy. Arrows indicate colocalization of NogoΔ20 with EEA-1. Bar, 10 μm. (D) Dissociated hippocampal neurons cultured for 4 d were incubated with 300 nM NogoΔ20-T7 for 30 min at 37°. NogoΔ20 (green) appears in vesicular structures in the cell body and neurites of the neurons, as indicated with arrowheads. NogoΔ20-positive vesicles colocalize with EEA-1 (red). The inset panel shows an enlarged view of the boxed region. Bar, 10 μm. (E) Quantification of colocalization of NogoΔ20 with EEA-1 after indicated time points. Values are given as the mean from three independent experiments ± SEM. (F) Subcellular fractionation of PC12 cells after internalization of NogoΔ20-T7 for 30 min at 37°C. Cells were homogenized and centrifuged to separate nuclei (NF, nuclear fraction) from the postnuclear supernatant, which was loaded on a 8–40.6% sucrose step gradient to separate different organelles. After centrifugation, different fractions F1 (8–25% sucrose), F2 (25–35% sucrose), and F3 (35–40.6% sucrose) were collected and immunoblotted for EEA-1 (top), nucleoporin p62 (middle), and NogoΔ20-T7 (bottom). A representative blot from three experiments is shown.

(Fish et al., 2000), in PC12 cells did not affect the internalization of NogoΔ20-T7 ($90.12 \pm 2.95\%$ vs. $99.93 \pm 7.61\%$ in control, $n = 303$ vs. 323 in control; Fig. 2, C and E). The internalization of transferrin, however, was almost completely inhibited ($4.86 \pm 1.67\%$ vs. $99.88 \pm 5.75\%$ in control, $n = 332$ vs. 216; ***, $P < 0.001$; Fig. 2, C and E).

Internalization via caveolae is cholesterol dependent. The cholera toxin β subunit (CTxβ) has been reported to be predominantly internalized through the cholesterol-sensitive pathway (Kirkham et al., 2005). To test the possibility that NogoΔ20-T7

internalization might depend on cholesterol, we pretreated PC12 cells with nystatin and progesterone. Combined cholesterol depletion by nystatin and inhibition of cholesterol synthesis by progesterone resulted in a significant inhibition of the uptake of cholera toxin β ($30.33 \pm 5.81\%$ vs. 99.40 ± 5.48 in control, $n = 478$ vs. 366; ***, $P < 0.001$; Fig. 2, D and E), whereas NogoΔ20-T7 endocytosis remained unaffected ($85.32 \pm 4.32\%$ vs. $99.93 \pm 7.61\%$ in control, $n = 487$ vs. 323; Fig. 2, D and E).

Collectively, these data provide strong evidence that internalization of NogoΔ20-T7 does not follow the conventional endocytic
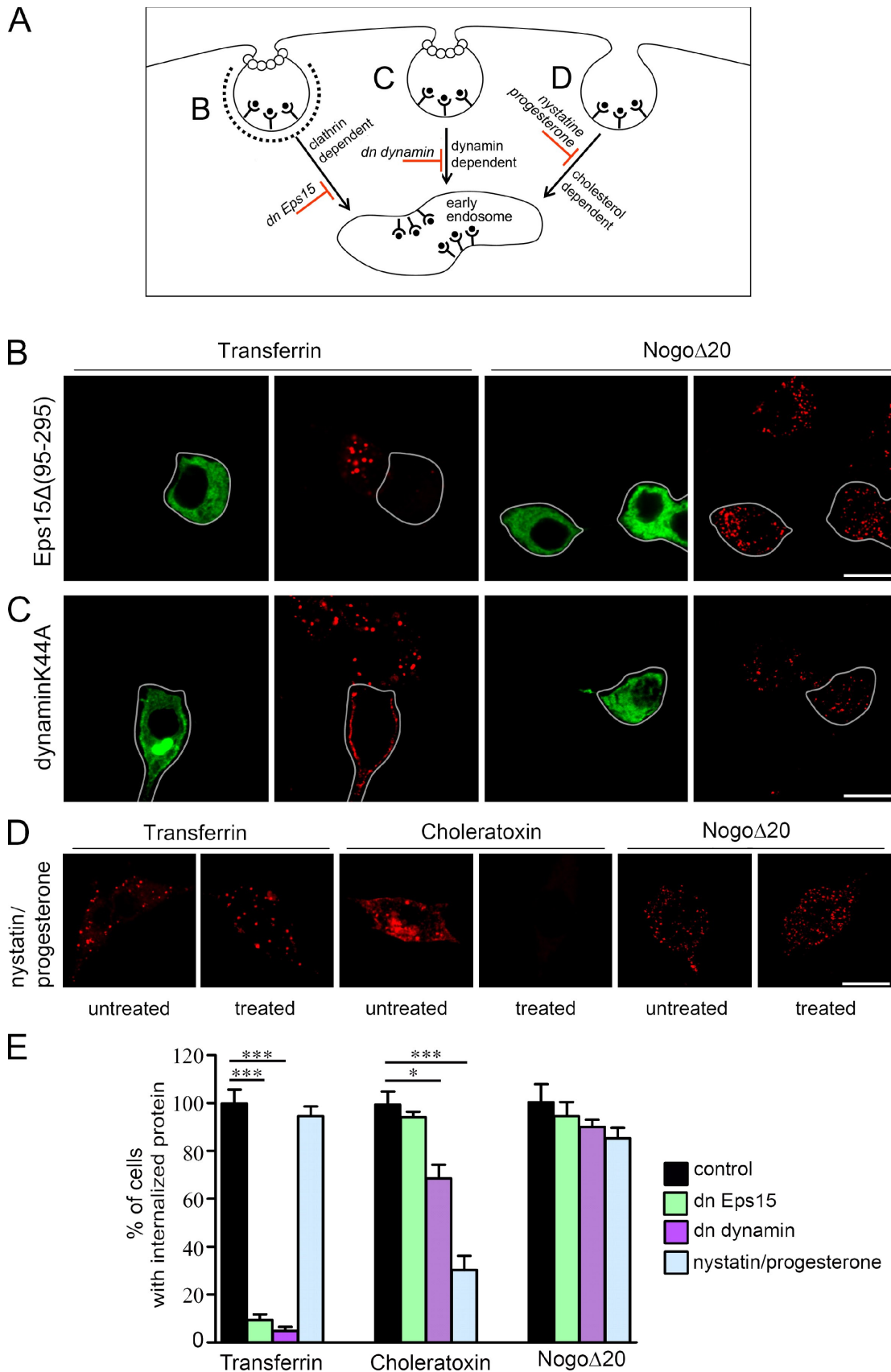
Figure 2.   **Internalization of NogoΔ20 occurs independently of Epsin15, dynamin II, and cholesterol.** (A) Schematic representation of different endocytotic pathways and their blockers. (B and C) PC12 cells were transfected with GFP-tagged Eps15Δ (95–295) (B, green), or GFP-dynIIK44A (C, green). 24 h later, cells were incubated with 300 nM NogoΔ20-T7 (red) or 100 nM transferrin-biotin (red) for 30 min at 37°C. In Eps15Δ (95–295) and dynIIK44A-transfected cells, transferrin uptake was blocked, but uptake of NogoΔ20 was not. White lines indicate the outlines of GFP-expressing cells. Bars, 10 µm.

routes. Neither clathrin, caveolin, nor cholesterol were required for the internalization of NogoΔ20-T7 into the PC12 cells.

NogoΔ20 endocytosis is mediated by Pincher-dependent macroendocytosis

The pinocytic chaperon protein Pincher belongs to the family of Eps15 homology (EH) domain–containing proteins (EHDs/RME-1), which have been implicated in clathrin-independent endocytosis (Shao et al., 2002; Valdez et al., 2007) and recycling from endosomes (Grant et al., 2001; Caplan et al., 2002). Overexpression of a dn form of Pincher (PincherG68E) has been shown to prevent NGF-induced internalization of TrkA (Shao et al., 2002). To assess a possible role of Pincher for NogoΔ20-T7 endocytosis, we overexpressed dn HA-PincherG68E in PC12 cells. In agreement with previous observations (Shao et al., 2002), HA-PincherG68E was associated with the plasma membrane in PC12 cells. Interestingly, the expression of dn Pincher dramatically reduced the endocytosis of NogoΔ20 (15.31 ± 3.68% vs. 99.46 ± 5.49% in control, n = 47 cells; ***, P < 0.001; Fig. 3, A and F). Confocal analysis revealed that NogoΔ20-T7 localization remained restricted to the plasma membrane and that 73.37 ± 2.91% of NogoΔ20-T7 colocalized with PincherG68E (Fig. 3, B and E). In contrast, transferrin was internalized and appeared in a punctate pattern in the cytoplasm of the PC12 cells, which is consistent with previous results showing that PincherG68E does not interfere with clathrin-mediated endocytosis (Shao et al., 2002). Accordingly, we observed only 9.74 ± 2.02% of transferrin overlap with PincherG68E (Fig. 3, B and E). These results indicate that Pincher function is essential for NogoΔ20 endocytosis.

The small GTPase Rac has been shown to drive the formation of membrane ruffles during macroendocytosis and thus to be required for Pincher-mediated NGF-TrkA internalization (Valdez et al., 2007). To test whether Rac is involved in NogoΔ20 internalization, we transfected PC12 cells with either wild-type (wt) Rac or the dn RacN17. The overexpression of RacN17 significantly blocked the internalization of NogoΔ20 (26.08 ± 4.45% vs. 99.46 ± 5.49% in control, n = 47 cells; ***, P < 0.001). As shown by confocal microscopy, NogoΔ20 remained at the plasma membrane of PC12 cells expressing RacN17 (Fig. 3, D and F). The overexpression of Rac1 had only a minor effect on the uptake of NogoΔ20 (77.64 ± 5.12% vs. 99.46 ± 5.49% in control, n = 47 cells; *, P < 0.05; Fig. 3, D and F). These findings strongly suggest that NogoΔ20 endocytosis is mediated by a macroendocytic process that depends on both Pincher and Rac proteins.

## Pincher-mediated NogoΔ20 endocytosis is required for NogoΔ20-induced growth cone collapse

NogoΔ20 is a very potent inducer of growth cone collapse that often leads to withdrawal of neurites (Niederöst et al.,

2002; Oertle et al., 2003). To determine the importance of NogoΔ20 endocytosis for the growth cone collapse, we examined the growth cone response of hippocampal neurons after blocking NogoΔ20 endocytosis. Dissociated E19 hippocampal neurons were infected with recombinant adenoviruses containing either HA-Pincher or HA-PincherG68E (Valdez et al., 2005). Growth cone collapse was assessed at 4 d in vitro (DIV), i.e., 48 h after viral infection by adding 300 nM of NogoΔ20 to the medium for 30 min. The neurons were fixed and the morphology of the growth cones was visualized by staining for F-actin with phalloidin–Alexa Fluor 488 (Fig. 4, A and B). The infected neurons were identified by visualization of the HA tag (Fig. 4 C). NogoΔ21 does not stimulate growth cone collapse at 300 nM; we thus used this fragment as a negative control. Three independent experiments (n = 109 neurons) showed that NogoΔ20 treatment induced collapse of 69.85 ± 2.55% of the growth cones as compared with 25.11± 1.59% observed after the NogoΔ21 control treatment (Fig. 4 C). A very similar proportion of growth cones, 67.23 ± 2.67%, collapsed if NogoΔ20 was added to the neurons overexpressing the Pincher protein (Fig. 4 F). In contrast, growth cone collapse induced by NogoΔ20 was fully abolished when PincherG68E was overexpressed. In this case, only 27.33 ± 1.79 of the growth cones showed a collapsed morphology (Fig. 4 F). To exclude possible nonspecific effects of PincherG68E, we assessed the growth cone collapse response to a well-known collapse-inducing protein, semaphorin 3A (Luo et al., 1993; He and Tessier-Lavigne, 1997; Kolodkin et al., 1997; Tamagnone et al., 1999). More than 70% of the growth cones collapsed after the addition of semaphorin 3A in Pincher as well as in PincherG68E-overexpressing hippocampal neurons; there was no significant difference (75.48 ± 2.54% and 70.06 ± 1.77%, respectively; Fig. 4 I) between the two treatments. These data strongly suggest that Pincher-dependent endocytosis is a crucial step in the chain of events that induce NogoΔ20-specific growth cone collapse.

In addition to the growth cone collapse assay, we tested the importance of Pincher-dependent NogoΔ20 endocytosis in a classical neurite outgrowth assay. Cerebellar granule neurons (CGNs) were infected with recombinant adenoviruses containing HA-PincherG68E for 24 h and plated onto 100 pmol of NogoΔ20-coated culture dishes. The neurons were fixed 24 h later, and the neurites were visualized by staining for neuronal microtubules with MAP1B. The infected neurons were identified by visualization of the HA tag (Fig. 4, J and K). The overexpression of mutant PincherG68E could partially overcome the inhibitory effect of NogoΔ20. CGNs overexpressing mutant PincherG68E exhibited 30% longer neurites than the control neurons without PincherG68E (32.29 ± 5.42% vs. 3.94 ± 1.69%; Fig. 4 L).

(D) PC12 cells were either left untreated or were pretreated with nystatin and progesterone overnight, and then incubated with transferrin, choleratoxin, or NogoΔ20-T7 for 30 min at 37°C in the absence or presence of drugs. Although the internalization of choleratoxin was inhibited (red), the internalization of transferrin (red) and NogoΔ20 (red) was not affected. Representative optical sections from three independent experiments are shown. Bar, 10 µm. (E) Quantification of protein uptake after various cell treatments. The percentage of cells with internalized protein is given as the mean ± SEM (*, P < 0.05; ***, P < 0.001; Student's t test).

Figure 3. Internalization of NogoΔ20 occurs by macroendocytosis and is Pincher and Rac1 dependent. (A) PC12 cells were transfected with HA-tagged dn PincherG68E (red). 24 h after transfection, cells were incubated with 300 nM NogoΔ20-T7 (green) for 30 min at 37°C. NogoΔ20 remained on the cell surface; no internalized NogoΔ20 vesicles are seen. (B) Transferrin (green) uptake is unaffected by overexpression of dn PincherG68E (red). (C and D) PC12 cells were transfected with T7-tagged wt Rac1 (C, red) or dn Rac1N17 (D, red) before incubation with 300 nM of Fc-tagged NogoΔ20 (green). After 30 min at 37°C, NogoΔ20 appeared in a large number of endosomal vesicles and cisterns inside the wt Rac1 cells (arrow), but the internalized proportion was reduced in the dn RacN17 transfected cells. Bar, 5 µm. (E) Quantification of NogoΔ20 and transferrin colocalization with dn PincherG68E. Values are given as the mean of three independent experiments ± SEM. (F) Quantification of internalization revealed that the uptake of NogoΔ20 was reduced by 84% upon overexpression of dn PincherG68E and by 73% upon overexpression of dn Rac1N17. Values are given as the mean from three independent experiments ± SEM (*, $P < 0.05$; ***, $P < 0.001$; Student's t test).
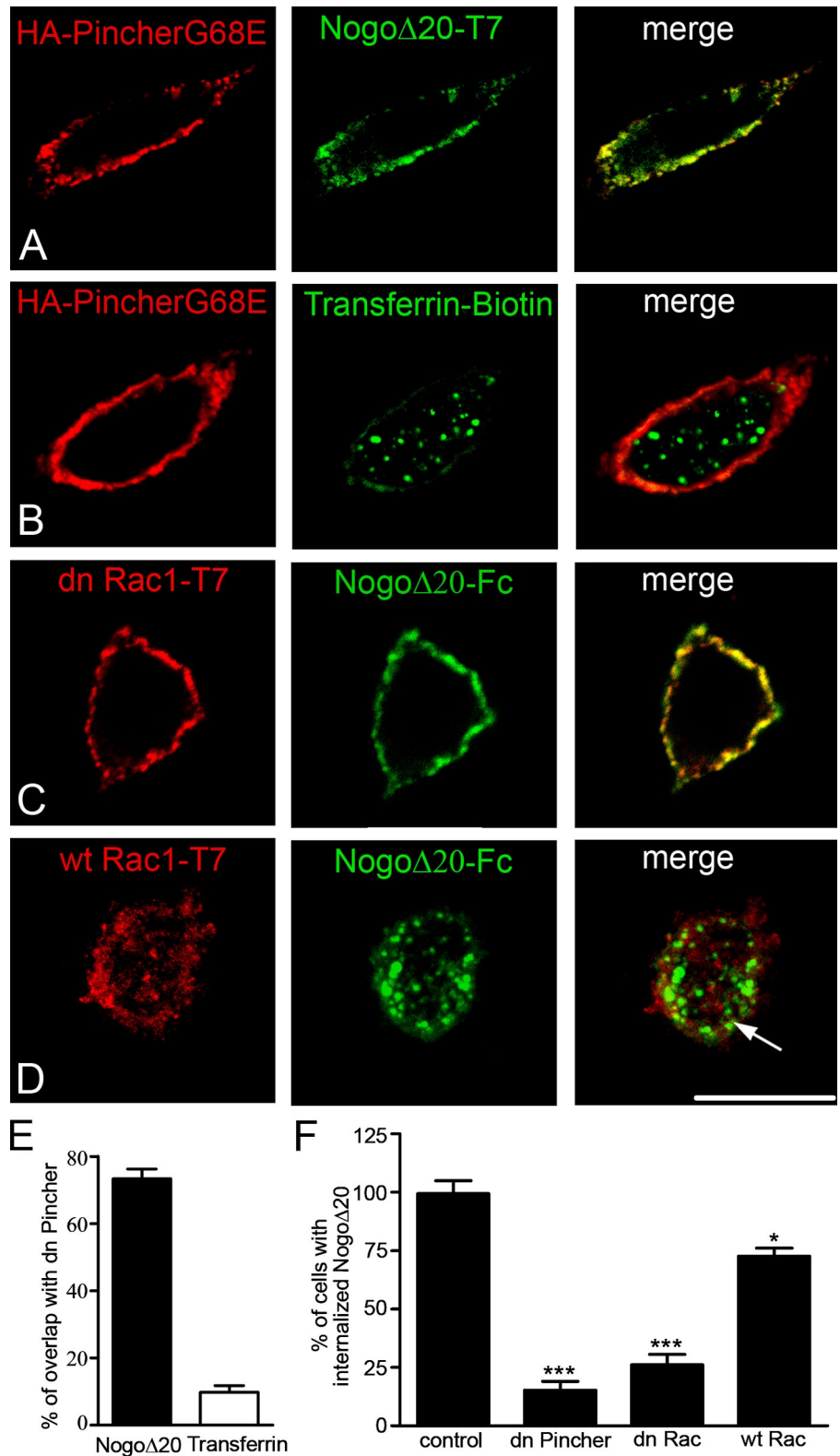
Inhibition of Pincher-dependent NogoΔ20 internalization reduces Rho activation

The Rho family of small GTPases, which includes Rho, Rac, and Cdc42, has important roles in regulating actin cytoskeletal dynamics. NogoΔ20 activates RhoA, thus leading to disassembly of the actin cytoskeleton during growth cone collapse and growth inhibition (Niederöst et al., 2002; Schwab, 2004). We investigated whether Rho activation could be dependent on NogoΔ20 internalization. To measure activated Rho, we used GST–Rhotekin–Rho-binding domain (RBD), which has been described to selectively bind to the active GTP-bound Rho proteins (Aspenström, 1999; Ren et al., 1999). NogoΔ20 (300 nM)

was added to PC12 cells for 30 min. Cells were then fixed, incubated with GST-Rhotekin-RBD, immunostained for GST, and quantified by densitometry. The comparison of the activated Rho levels of nontreated (Fig. 5 A) versus NogoΔ20-treated (Fig. 5 B) cells revealed a dramatic increase of Rho activation upon NogoΔ20 addition (1.49 ± 0.03 vs. 1.00 ± 0.02 in control, $n = 149$ vs. 137 cells; ***, P < 0.001; Fig. 5 D). However, when the macroendocytosis was blocked by the overexpression of dn PincherG68E (Fig. 5 C), activation of Rho in PC12 cells remained at background levels after addition of NogoΔ20 (1.12 ± 0.04 vs. 1.00 ± 0.02 in control, $n = 98$ vs. 137 cells; Fig. 5 D). Reduced RhoA activation (23.12 ± 4.63% of control, $n = 3$ independent experiments) in cells overexpressing dn PincherG68E was confirmed in the RhoA pull-down assay (Fig. 5 E). This finding that inhibition of NogoΔ20 internalization interferes with Rho activation suggests that NogoΔ20-containing vesicles may function as signalosomes, as described, e.g., for NGF (Howe et al., 2001; Delcroix et al., 2003).

Internalized NogoΔ20 is retrogradely transported from neurites to cell bodies

To further test the role of Nogo-Δ20 endosomes, we examined whether NogoΔ20 could be retrogradely transported from the axons to the cell bodies. Dissociated DRG cells from E19 rats were cultured in compartmentalized chambers (Campenot, 1977), as indicated in Fig. 6 A. Within 7 d, fascicles of neurites grew under the Teflon ring and silicon grease seals into the two side chambers and established a dense neuritic plexus. NogoΔ20-T7 (300 nM) was then added to the side chambers. After 30 min or 6 h, NogoΔ20 was visualized by confocal microscopy. After 30 min of incubation, NogoΔ20 fluorescence appeared in vesicular structures in the neurites of the distal compartments (Fig. 6, B and C) but was not detectable in proximal neurites and the cell bodies (Fig. 6, D and E). In contrast, after 6 h of incubation, a large number of NogoΔ20-containing vesicles appeared in proximal neurites and the cytoplasm of DRG cell bodies (Fig. 6, F and G), which indicates the retrograde movement of endocytosed NogoΔ20 from the neurites in the side chambers to the cell bodies in the center chamber of the culture. Although the majority of the cell bodies were positive for NogoΔ20 (62.18 ± 6.74%, $n = 4$ independent experiments), some of the DRG cell bodies remained unlabeled (37.82 ± 3.36%), showing that the fluorescent signals did not derive from leakage and direct uptake by cell bodies. Importantly, the blockade of retrograde transport with colchicine (Kreutzberg, 1969) completely abolished NogoΔ20 detection in the DRG cell bodies, which shows the involvement of active microtubule-dependent transport during NogoΔ20 trafficking from the axons to the cell bodies (Fig. S2, A–C).

As Pincher plays a crucial role in NogoΔ20 endocytosis in PC12 cells, we analyzed the requirement of Pincher function on uptake and retrograde transport of NogoΔ20 in DRG neurons. No NogoΔ20 could be detected in the cell bodies of those DRG neurons overexpressing PincherG68E (Fig. S2, D and E). The overexpression of PincherG68E completely abolished the retrograde trafficking of NogoΔ20, which confirms that the Pincher protein is required for neuronal Nogo-A uptake and trafficking.

Retrogradely transported NogoΔ20 activates RhoA en route and decreases pCREB levels in the DRG cell bodies

Next, we asked if Rho activation can be observed in DRG neurites and cell bodies after internalization of NogoΔ20. Active Rho was measured with GST-Rhotekin-RBD protein, as described earlier in the distal neurites and in the cell bodies of the compartmentalized DRG cultures, 30 min and 6 h after addition of 300 nM NogoΔ20 to the distal neurite compartments. We found Rho activation in the neurite compartments 30 min after NogoΔ20 addition. Interestingly, active Rho was precisely colocalized with NogoΔ20-positive vesicles in the neurites (Fig. 7, A–C; 86.58 ± 14.48% of overlap, $n = 26$ neurites). In the cell body compartment, the Rho activation was not seen at 30 min (Fig. 7, D and E) but was prominent at 6 h after NogoΔ20 addition to the neurites (Fig. 7 G). Thus, the temporal activation of RhoA reflects the retrograde transport of NogoΔ20, which suggests the formation of NogoΔ20/RhoA signalosomes. To further test the signalosome hypothesis, endosomal fractions were isolated from PC12 cells with and without prior addition of NogoΔ20 and analyzed for their active RhoA content. Endosomal fractions from NogoΔ20-treated cells exhibited higher levels of activated RhoA compared with endosomal fractions from naive PC12 cells (Fig. 7 I). These data suggest that NogoΔ20 initiates the recruitment and assembly of specific signaling components, including the small GTPAse RhoA, to so-called "NogoΔ20 signalosomes."

The activation of the cAMP response element–binding protein CREB, e.g., by neutrophins, can overcome inhibitory effects of myelin-associated neurite outgrowth inhibitors (Gao et al., 2004). To test whether NogoΔ20 influences CREB signaling, we determined the levels of pCREB upon NogoΔ20 addition. The low basal level of pCREB in DRG cell bodies makes these neurons highly responsive to increases in pCREB, which occurs after application of neutrophins to the axons (Watson et al., 1999). Because our DRG neurons are cultured in compartmentalized chambers in the presence of NGF, we detected high basal levels of pCREB (Fig. 7 J). The addition of NogoΔ20 to the distal compartments for 6 h resulted in a marked decrease (22.39 ± 4.47% of control, $n = 3$ experiments) of pCREB in the cell body compartment (Fig. 7 J).

To address whether activation of CREB is sufficient to overcome inhibition of NogoΔ20, we analyzed the neurite outgrowth of CGNs on different concentrations of NogoΔ20 in the presence or absence of 1 mM dibutyryl cAMP (db-cAMP). The addition of db-cAMP elevated pCREB levels (27.23 ± 3.19% of untreated condition, $n = 3$ experiments; Fig. 8 D) and almost completely overcame NogoΔ20 neurite outgrowth inhibition even at high NogoΔ20 concentration (Fig. 8 E), which suggests a mechanistic link between NogoΔ20 and pCREB.

Discussion

So far, studies on endocytosis and retrograde transport of ligand–receptor complexes in neurons have focused on factors promoting survival and growth, in particular the neutrophins (Ginty and Segal, 2002; Campenot and MacInnis, 2004; Howe
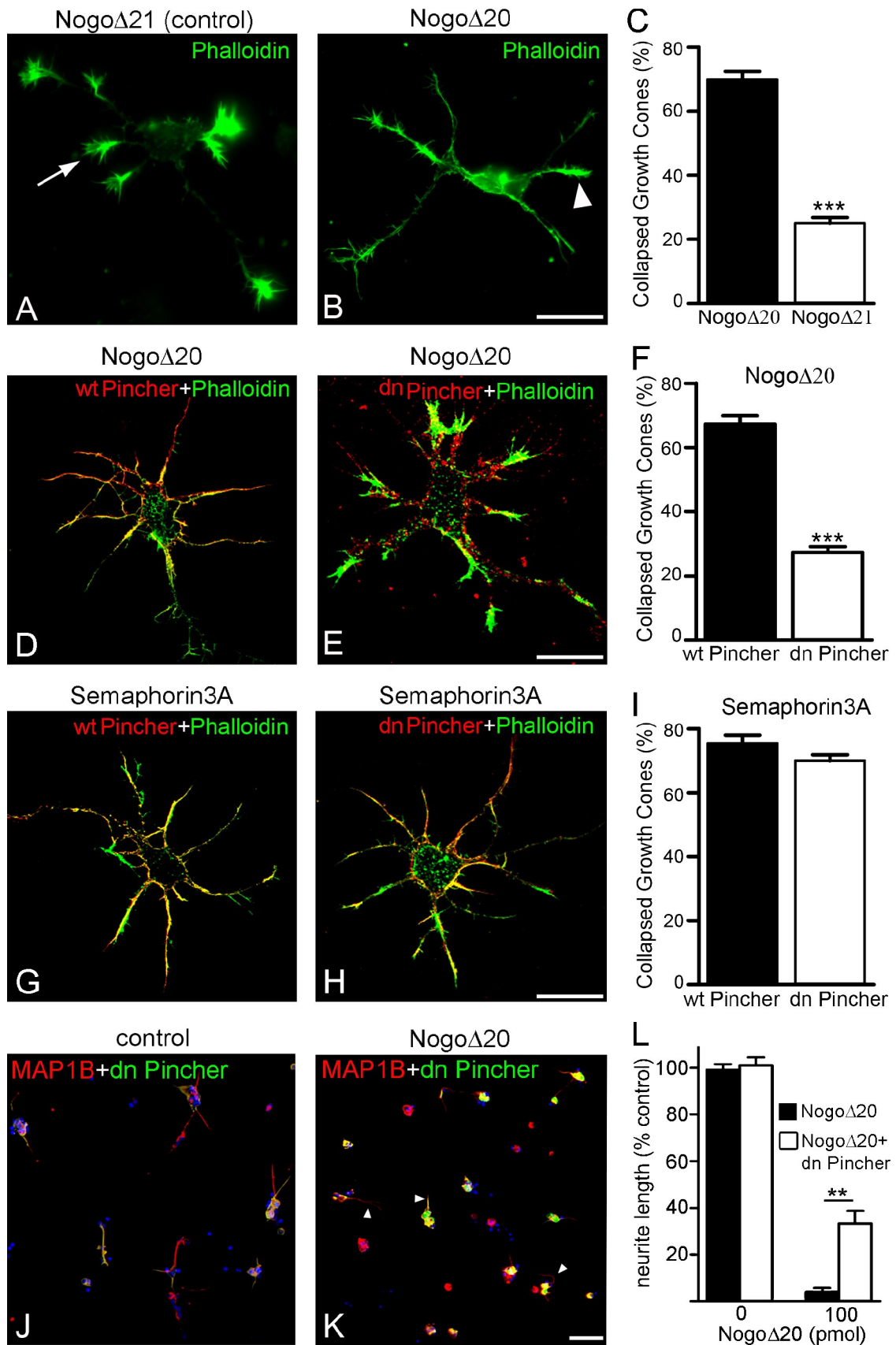
Figure 4. **Endocytosis of NogoΔ20 is required for NogoΔ20-induced growth cone collapse in hippocampal neurons.** (A and B) Morphology of non-collapsed (A, arrow) and collapsed growth cones (B, arrowhead) of E19 hippocampal neurons at DIV 4 was visualized by staining of F-actin with phalloidin–Alexa Fluor 488 (green). (C) Quantification of the proportion of collapsed growth cones after incubation with 300 nM NogoΔ20 (shaded bars) or with
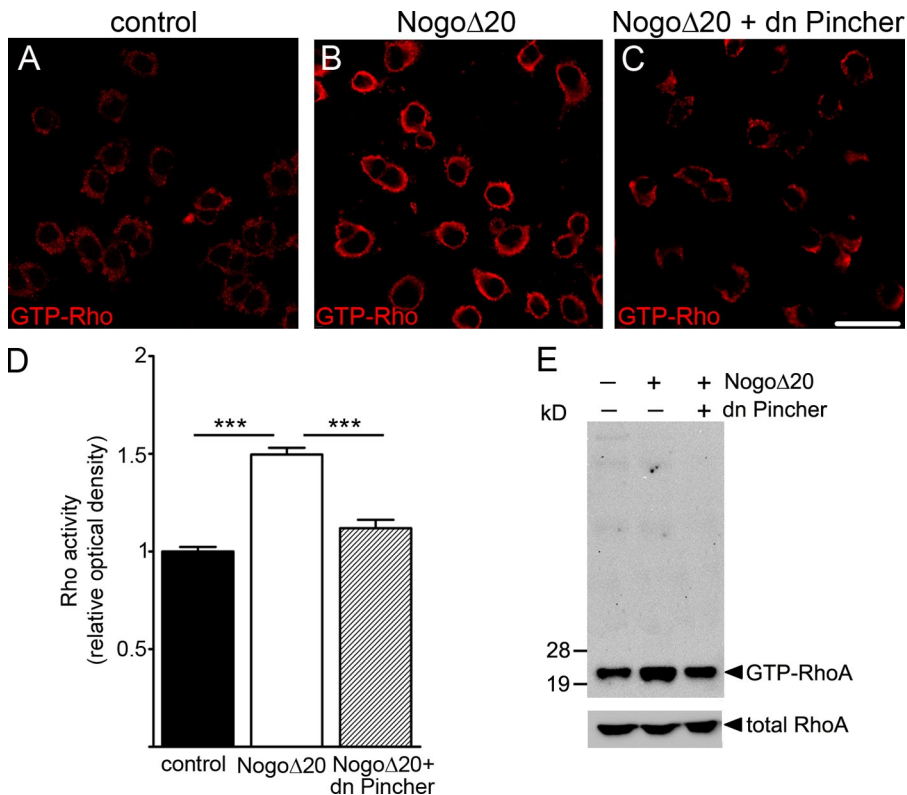
Figure 5. NogoΔ20-induced Rho activation depends on internalization. (A–C) Rho activation levels were examined in PC12 cells that were either untreated (control; A), treated with 300 nM NogoΔ20 for 30 min at 37°C in absence of mutant PincherG68E (B), or treated with 300 nm Nogo Δ20 treated for 30 min at 37°C in the presence of mutant PincherG68E (C). Active GTP-bound Rho was detected by incubation with GST-tagged Rhotekin-RBD and immunostaining. Bar, 20 µm. (D) Densitometric quantification of staining from three independent experiments. Data are normalized to the mean of the untreated group ± SEM (error bars); asterisks marks highly significant differences between untreated, NogoΔ20-treated, or NogoΔ20- and dn PincherG68E-treated cells (three experiments; 30–50 cells per experiment; ***, P < 0.001; Student's *t* test). (E) PC12 cells were either left untreated or transfected with dn PincherG68E construct. All cells were then incubated with 300 nM NogoΔ20 for 30 min at 37°C. Extracted proteins were precipitated with Rhotekin-RBD beads. Precipitates were immunoblotted for RhoA (top). Total RhoA levels were determined from whole cell lysates as shown in the bottom panel.

and Mobley, 2005). However, during development and in the adult nervous system, neurons are also exposed to growth inhibitory signals, a prominent one being Nogo-A. Up to now, nothing was known about whether the neurite growth inhibitors like Nogo-A can signal through endosomes, which may also be retrogradely transported in neurons. We used NogoΔ20, the most potent fragment of Nogo-A that mediates growth cone collapse through a receptor other than NgR, to examine the role and mechanism of endocytosis. We found that NogoΔ20 is endocytosed in a nonconventional manner, using Pincher- and Rac-mediated macroendocytosis. Endocytosis of NogoΔ20 is essential to mediate growth cone collapse: inhibition of Pincher-mediated NogoΔ20 endocytosis prevented NogoΔ20-induced, but not semaphorin 3A–induced, growth cone collapse and diminished NogoΔ20-triggered RhoA activation. Furthermore, NogoΔ20 is taken up by DRG neurites and retrogradely transported to the cell bodies, where it activates Rho and reduces pCREB levels, which suggests that NogoΔ20 signalosomes transmit growth-inhibitory signals from the neurites to the soma.

Most cell surface proteins and receptor-bound ligands are internalized through the clathrin-coated vesicle or the caveolin pathways (Le Roy and Wrana, 2005; Mayor and Pagano, 2007). We found that NogoΔ20 internalization does not depend on the Nogo66 receptor NgR, as shown by pharmacological blockage of NgR with PI-PLC or NEP1-40. Surprisingly, neither cholesterol depletion nor overexpression of the dn constructs Eps15 EΔ95/295 and dynamin K44A, which interfere with the clathrin and caveolin endocytosis machinery, were able to abolish NogoΔ20 endocytosis. Pincher protein has recently been classified as a member of the dynamin superfamily (Daumke et al., 2007) and mediates the clathrin-independent, Rac-mediated, and pinocytosis-like uptake of the activated neurotrophin receptor complex (Shao et al., 2002). Overexpression of a mutant form of the Pincher protein in which the P-loop ATP-binding site was destroyed by G68E mutation (Shao et al., 2002) almost completely blocked the internalization of NogoΔ20, which indicates a requirement of Pincher ATPase activity for this process. The requirement for Pincher protein and the small GTPAse Rac for NogoΔ20 internalization

300 nM NogoΔ21 (open bars). (D and E) The morphology of hippocampal neurons infected with immunodeficient recombinant adenovirus containing HA-tagged wt Pincher (D, red) or HA-tagged dn PincherG68E (E) upon treatment for 30 min with 300 nM NogoΔ20 was visualized with phalloidin (green). (F) Most growth cones remained uncollapsed when HA-tagged dn PincherG68E was overexpressed (open bars) compared with wt Pincher (shaded bars). (G and H) Growth cone morphology of hippocampal neurons upon treatment with 40 nM semaphorin 3A overexpressing either wt HA-Pincher protein (G) or dn HA-PincherG68E protein (H). (I) Treatment with 40 nM semaphorin 3A for 30 min leads to growth cone collapse in the presence of both wt HA-Pincher (shaded bars) and dn HA-Pincherg68E (open bars). Data represent the mean of three (semaphorin 3A) or four (NogoΔ20) independent experiments ± SEM (90 neurons per group and experiment). Asterisks mark highly significant differences between wt and dn Pincher-infected hippocampal neurons (***, P < 0.001; Student's *t* test). (J and K) CGNs infected with immunodeficient recombinant adenovirus containing HA-tagged dn PincherG68E (green) were plated on either uncoated plates (J) or with 100 pmol coated NogoΔ20 plates (K), and visualized with the neuronal marker MAP1B (red) and DAPI (blue) upon they were cultured for 24 h. Arrowheads in K indicate long neurites in the presence of mutant Pincher G68E. (L) The mean neurite length was measured and normalized to the mean of the control (without NogoΔ20) group. Overexpression of the mutant PincherG68E only partially overcomes the neurite outgrowth inhibitory effect of NogoΔ20. Asterisks mark significant differences between untreated and mutant PincherG68E-overexpressing cells (three experiments; 40–60 cells per experiment; **, P < 0.01; Student's *t* test). Bars: (H) 10 µm; (K), 20 µm.

Figure 6. **Upon internalization, NogoΔ20 is retrogradely transported from the neurites to the cell bodies of dissociated DRG neurons.** (A) Schematic representation of a compartmentalized chamber. (B–F) Representative immunofluorescence images of retrogradely transported NogoΔ20 (300 nM) at indicated time points in dissociated DRG neurons that were cultured in compartmentalized Campenot chambers. (B) Uptake of NogoΔ20 (green) in the distal neurites at 30 min of incubation. Bar, 20 µm. (C) NogoΔ20-positive vesicles (green, arrowhead) in the distal neurites. Bar, 10 µm. (D) NogoΔ20 could not be observed in the cell body compartment 30 min after NogoΔ20 addition. (E) Cell bodies were stained with DAPI (blue). Bar, 40 µm. (F and G) NogoΔ20-positive distal neurites (F) and cell bodies (G) 6 h after addition of NogoΔ20 to the distal compartment. The arrowhead indicates NogoΔ20-positive vesicles in the cell body. The inset panels in C and G show enlarged views of the boxed regions. Bars, 20 µm.
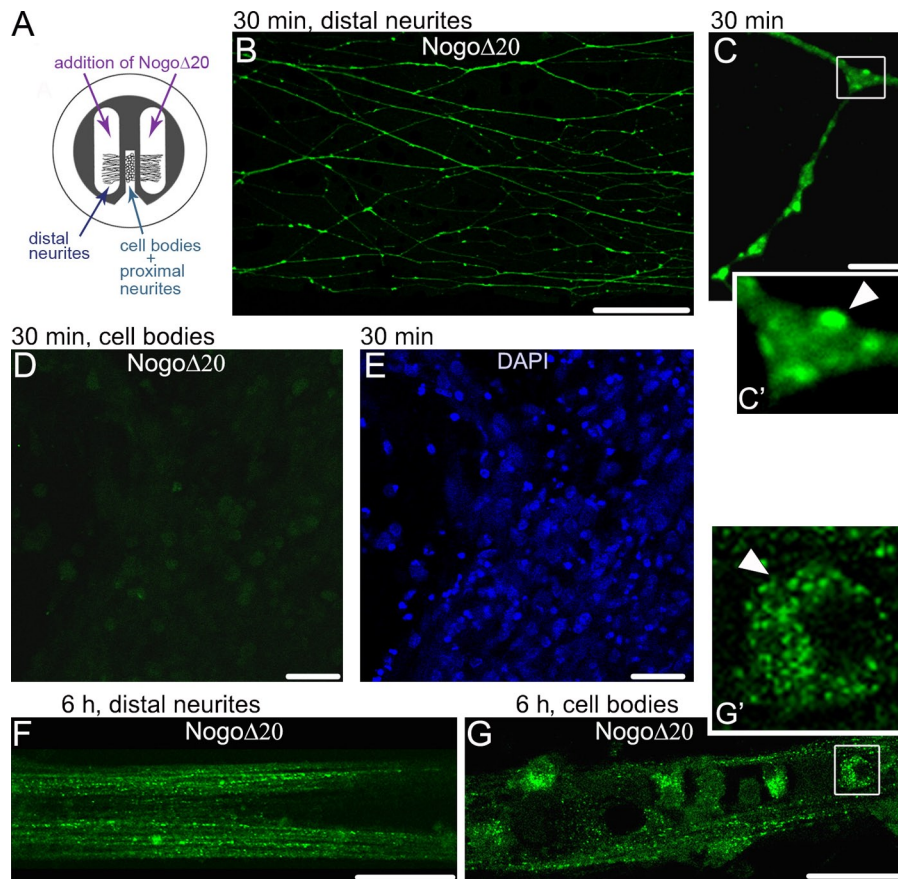
leads to the conclusion that NogoΔ20 is taken up by macroendocytosis, similar to NGF. Macroendocytic signaling may have more general implications in growth inhibition because EphrinB-EphB–containing vesicles also do not colocalize with the known markers of the clathrin and caveolin endocytic pathways (Marston et al., 2003); they may also be internalized via Rac-dependent macroendocytosis (Marston et al., 2003).

Using growth cone collapse as a functional readout, we addressed the question of whether NogoΔ20 internalization is necessary for NogoΔ20 signaling. Blockade of NogoΔ20 endocytosis by dn PincherG68E prevented NogoΔ20-induced growth cone collapse of hippocampal neurons. Under the same conditions, semaphorin 3A–induced growth cone collapse was not affected. Importantly, the NogoΔ20-induced growth cone collapse is known to occur with a slower time course than the collapse elicited by semaphorin 3A (Oertle et al., 2003), which suggests different signaling cascades evoked by the two proteins. For Nogo-A, the first morphological changes can be observed after 90 s, and the collapse is complete after 20–40 min (Bandtlow et al., 1993; Oertle et al., 2003). Interestingly, this time course matches that of NogoΔ20 endocytosis: first, NogoΔ20-containing vesicles appeared after 2 min of exposure to NogoΔ20 (unpublished data), and a large number of NogoΔ20 endosomes accumulated intracellularly after 30 min. This slow time course of endocytic processing is similar to that found for the neurotrophins, as opposed to, e.g., epidermal growth factor receptor (EGFR) endocytic signaling, and may be a general feature of Pincher-mediated endocytic signaling (Valdez et al., 2007).

Importantly, members of another repulsive protein family, the ephrins, were also shown to depend on endocytosis for growth cone collapse: In the absence of Vav proteins, ephrin-Eph endocytosis was blocked, resulting in defects in growth collapse in vitro and significant defects in retinogeniculate axon guidance in vivo (Cowan et al., 2005).

Our finding that prevention of NogoΔ20 internalization also blocked the activation of Rho proteins in PC12 cells and DRG neurons provides a second line of evidence that NogoΔ20 internalization is required for NogoΔ20 signal propagation. Accordingly, subcellular fractionation revealed that NogoΔ20-containing early endosomes contain activated RhoA-GTPase, which indicates that NogoΔ20 signals after internalization. Consistent with this, we found that NogoΔ20-containing vesicles were transported retrogradely from the neurites to the cell bodies of DRG neurons cultured in compartmentalized chambers. Activated Rho colocalized with NogoΔ20-positive vesicles in these DRG neurites. As high Rho activity in the DRG cell bodies was not observed after 30 min but was observed prominently after 6 h of NogoΔ20 addition, we conclude that NogoΔ20 vesicles also activate Rho en route and after arrival in the cell bodies. Collectively, these data strongly show the formation of NogoΔ20 signaling endosomes, which are retrogradely transported along the axons.

Because NogoΔ20 is highly inhibitory for neurite outgrowth, we also assessed the role of Pincher-mediated endocytosis in a classical neurite outgrowth assay, where neurons (cerebellar granule cells) are plated onto NogoΔ20-coated culture dishes. We found that a blockade of NogoΔ20 endocytosis by dn PincherG68E
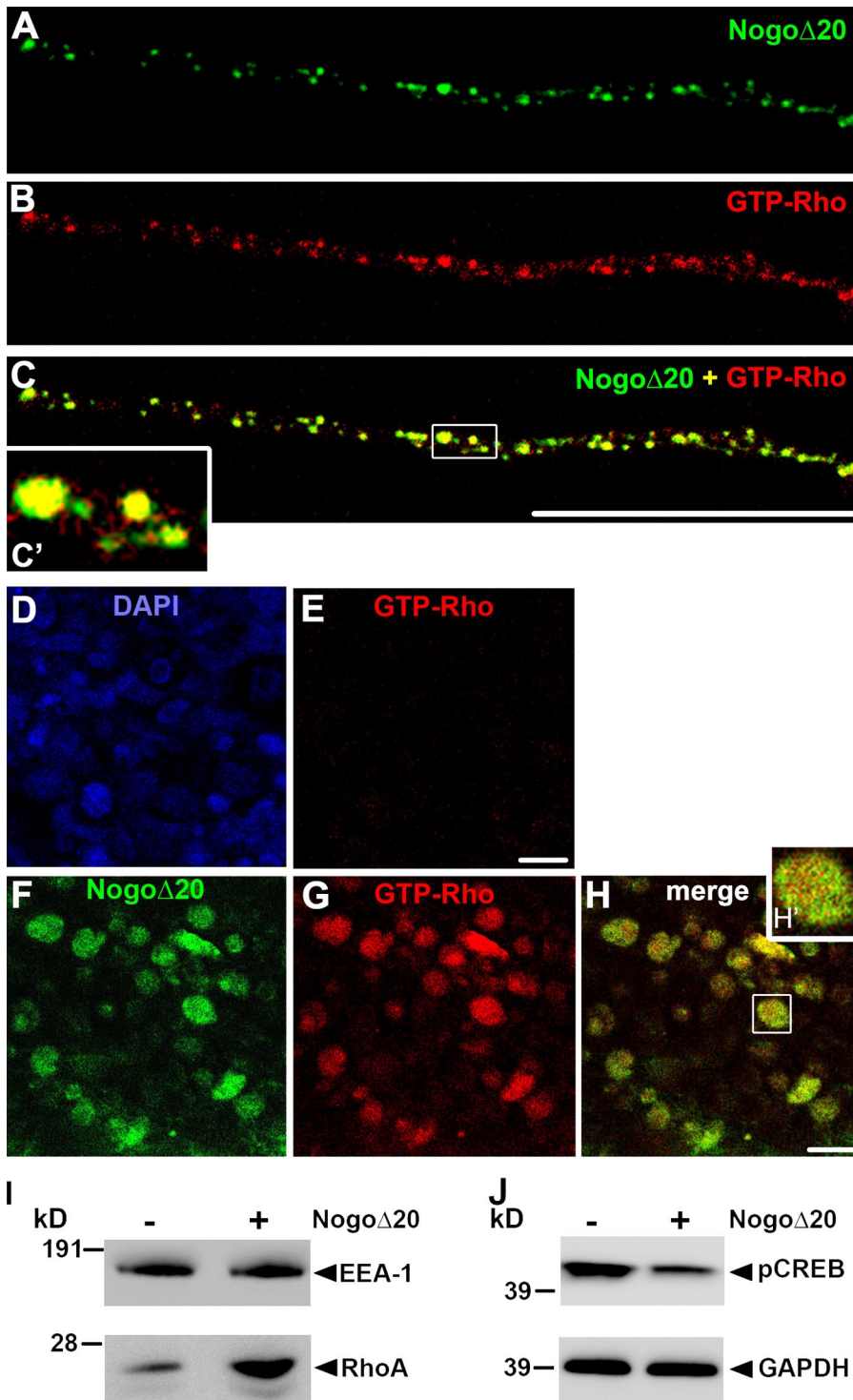
Figure 7. **NogoΔ20 triggers Rho activation en route to DRG cell bodies.** Active GTP-bound Rho was visualized in the distal neurites and the cell body compartment of Campenot chambers upon addition of NogoΔ20 (300 nM) to the distal compartment for either 30 min or 6 h. (A–C) 30 min after NogoΔ20 addition, activated Rho (red) colocalizes with NogoΔ20-positive vesicles in the neurites of the distal compartment of the Campenot chambers. The inset panel shows an enlarged view of the boxed region. (D and E) Cell bodies stained with DAPI (D, blue) were negative for activated Rho (E, red). (F–H) 6 h upon NogoΔ20 (green) addition, activated Rho (red) was also observed in the cell body compartment. The inset panel shows an enlarged view of the boxed region. Bars, 10 µm. (I) Early endosomes containing F1 sucrose density fractions of untreated (control) or NogoΔ20-treated (30 min at 37°C) PC12 cells were reacted with Rhotekin-RBD beads. The bound proteins were immunoblotted with an anti–Rho A monoclonal antibody (bottom). (J) Cell bodies from DRG neurons cultured in Chambers were collected 6 h after NogoΔ20 addition and immunoblotted for pCREB. The addition of NogoΔ20 decreased the pCREB levels.

could partially overcome the inhibitory effect of NogoΔ20. These data suggest that NogoΔ20 is released from the substrate to be taken up and act on the growing neurites.

In vivo, Nogo-A is predominantly found in the innermost, adaxonal membranes around axons in the intact CNS (Huber et al., 2002; Wang et al., 2002). One question that arises from our study is whether Pincher-dependent macroendocytosis occurs in vivo. Ephrins can be taken up by transcytosis of entire membrane domains (Zimmer et al., 2003); full-length Nogo-A could be internalized by a similar transcytotic event. Alternatively, Nogo-A could undergo protease-dependent cleavage resulting in the release of active fragments like NogoΔ20, which are then taken up by growth cones or axons. Several types of proteases are released by growing axons (Monard, 1988). The contact-mediated axon repulsion of, e.g., ephrins, is regulated by the protease Kuzbanian (Hattori et al., 2000). Similarly, the neurite outgrowth function of netrin-1 is modulated by proteolytic activity (Galko and Tessier-Lavigne, 2000). The existence of

Figure 8. Elevated pCREB levels can overcome neurite outgrowth inhibition of NogoΔ20. (A–C) CGNs were visualized with the neuronal marker MAP1B (red) and DAPI (blue) after they were cultured for 24 h either without treatment (A), on NogoΔ20 substrate (B), or on NogoΔ20 substrate in the presence of 1 mM db-cAMP (C). (D) CGNs were cultured either in the presence or absence of 1 mM db-cAMP for 24 h and subjected to Western blotting. Treatment of CGNs with 1 mM db-cAMP results in increased pCREB levels. Bar, 20 µm. (E) CGNs were cultured on different concentrations of substrate-bound NogoΔ20. The mean neurite length was measured either in the absence (shaded bars) or presence of 1 mM db-cAMP (open bars). The addition of db-cAMP can significantly overcome the inhibitory effect even at high NogoΔ20 concentrations. Data are normalized to the mean of the untreated group ± SEM (error bars); asterisks marks highly significant differences between untreated cells and db-cAMP–treated cells (three experiments; 50–70 cells per experiment; **, P < 0.01; ***, P < 0.001; Student's t test).
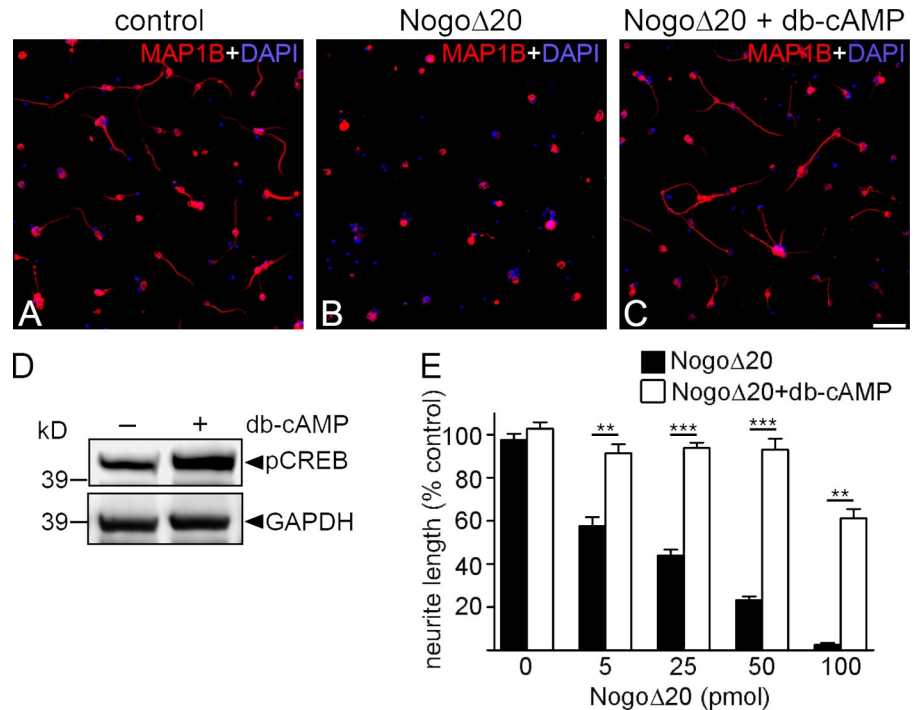
soluble Nogo-A fragments in cerebrospinal fluid from patients with multiple sclerosis (Jurewicz et al., 2007) and the cleavage of Nogo-A upon optic nerve injury (Ahmed et al., 2006) speak in favor of such a mechanism.

Given our finding that Nogo-A signals retrogradely, it is tempting to speculate that in the intact adult CNS, Nogo-A signals originating along the axons tonically suppress axonal growth. Once the axon has reached its target and myelination starts, Nogo-A starts to retrogradely communicate to the cell body that the growth machinery is not needed any longer and that outgrowth and branching in white matter tracts is unwanted. Indeed, acute injections of function-blocking antibodies into adult cerebella or CNS of rats induce transitory sprouting of Purkinje axons and the corticospinal tract (Buffo et al., 2000; Bareyre et al., 2002; Gianola et al., 2003). These findings support the concept of Nogo-A acting as an "end-of-growth" and stabilization signal in the maturing and adult CNS.

In many respects, Nogo-A seems to counteract the effect of neutrophic factor signaling. Although, e.g., NGF promotes neurite outgrowth and attracts growth cones, Nogo-A inhibits outgrowth and induces growth cone collapse. Retrograde trafficking of NGF signaling endosomes is associated with an increase in pCREB in cell bodies (Riccio et al., 1997; Cox et al., 2008). In contrast, we find that retrograde trafficking of NogoΔ20 is associated with a decrease of pCREB levels. The elevation of pCREB levels could overcome the inhibitory effect of NogoΔ20. Both proteins use a similar endocytic machinery, but achieve their opposing cellular responses through their specific ligand–receptor complexes and the retrogradely activated genes. Growth-enhancing neurotrophins and growth inhibitors like Nogo-A may therefore function as signals from the environment of the axons to regulate the growth homeostasis of the neuron in a yin–yang way.

Materials and methods

Cell culture

PC12 cells were grown in DME media (Invitrogen) supplemented with 6% newborn calf serum and 6% horse serum. Cells were transfected with Lipofectamine 2000 (Invitrogen) in OptiMEM (Invitrogen).

Primary hippocampal neurons derived from rat embryos were cultured as described previously (Kaech and Banker, 2006). In brief, the hippocampi of E19 rats were dissected, digested (0.05% papain; Sigma-Aldrich), and washed in PBS. Cells were then dissociated, and 6,000–8,000 cells were plated onto poly-L-lysine– and laminin-coated 18-mm glass coverslips in 12-well cell culture plates containing a glial feeder layer in neurobasal/B27 medium (Invitrogen).

Dissociated DRG neurons derived from E19 rats were cultured in Campenot chambers as described previously (Campenot, 1977). In brief, E19 dissociated DRG neurons were plated in the cell body compartment in neurobasal/B27 medium supplemented with 100 ng/ml NGF and 250 µM cytosine arabinoside (1-β-D-arabinofuranosylcytosine) to inhibit glial growth. At DIV 4, media was changed and compartments were checked for bulk leakage. Cultures from leaking chambers were excluded from further study. Retrograde transport experiments were performed at DIV 7, when neurites had crossed the divide into the distal neurite compartment.

Neurite outgrowth assays with postnatal day 4–6 rat cerebellar granule cells were performed as described previously (Niederöst et al., 1999).

DNA and viral constructs

Dynamin II K44A-GFP construct was obtained from M. McNiven (Mayo Clinic, Rochester, MN), the Eps15Δ(95–295)-GFP construct was obtained from A. Benmerah and A. Dautry-Varsat (Institut Pasteur, Paris, France), and Rac1-T7 (wt and N17 mutant) constructs were obtained from D. Bar-Sagi (New York University, New York, NY).

Defective adenoviruses containing Pincher-HA (Shao et al., 2002) constructs were used. For efficient infection, an MOI of 50 was used. Hippocampal neurons were infected at DIV 2 and analyzed at DIV 4. The cell body compartments of dissociated DRG neurons were infected at DIV 5 and the cultures were grown for further 2 DIV to achieve high level of protein overexpression.

Drug treatments

Cells were preincubated for 60 min at 37°C in serum-free DME containing 1 U/ml PI-PLC (Invitrogen) or 1 µM NEP1-40 (Alpha Diagnostic International, Inc.). Preincubation with 25 µg/ml nystatin (Sigma-Aldrich) plus

10 µg/ml progesterone (Sigma-Aldrich) was performed overnight. The drugs were present throughout the experiments. Cell bodies of DRG neurons were preincubated with 125 µM colchicine (Sigma-Aldrich) 1 h before addition of NogoΔ20.

Growth cone collapse

The response of neuronal growth cones was quantified on three independent experiments ($n = 90$ neurons per group from each experiment). At DIV 4, hippocampal neurons were incubated with either 300 nM NogoΔ21 (control), 300 nM NogoΔ20, or 40 nM semaphorin 3A for 30 min at 37°C, then fixed and stained for F-actin with phalloidin–Alexa Fluor 488 to visualize the growth cone morphology. The collapsed growth cones of each neuron, which were defined as those with no lamellipodia and not more than two filopodia (Kapfhammer et al., 2007), were counted and expressed as the percentage of the total growth cones of the belonging neuron. The infection with defective adenoviruses containing HA-Pincher constructs was performed at DIV 2 with 50 MOI. After 1 h, medium containing adenoviruses was removed and the cells were cultured for another 2 DIV before the collapse experiment. Only HA-Pincher–positive neurons, which were detected with anti-HA immunostaining, were analyzed in the growth cone collapse experiment.

Internalization assay and immunofluorescent microscopy

For internalization assays, PC12 cells were serum starved 3 h before the addition of proteins for 30 min at 37°C. Proteins were used at the following concentrations: NogoΔ20 and NogoΔ21 at 300 nM, transferrin-biotin (Invitrogen) at 1 µg/ml, and cholera toxin β-A594 (Invitrogen) at 1 ng/ml. Cells were then fixed with 4% paraformaldehyde for 15 min, surface stripped, and subsequently permeabilized with 0.1% Triton X-100 for 30 min at RT. After blocking, cells were incubated first with primary antibodies for 30 min, washed three times for 5 min, and then incubated with secondary antibodies for 30 min.

Coverslips were mounted with mounting medium (Dako). Images were acquired on a microscope (DM RE; Leica) using a confocal scanning system (SP2 or SP5; Leica) equipped with 40×/1.25 NA, 63×/1.4 NA, and 100× Plan-Chromat objectives. The thickness of all confocal slices varied between 0.2 and 0.8 µm.

Images were processed with the use of Photoshop (Adobe). Colocalizations were analyzed with the colocalization module of Imaris (Bitplane). Data were given as the mean value ± SEM. Data analysis was performed by Prism 4.0 (GraphPad Software) using an independent Student's t test.

The following primary antibodies were used: 1:250 rabbit anti–EEA-1 (Abcam), 1:1,000 mouse anti-T7 (EMD), 1:1,000 rabbit anti-Pincher (Shao et al., 2002), 1:250 rat anti-HA (Roche), and 1:250 mouse anti-MAP1B (Millipore). Secondary antibodies used were Alexa Fluor 488, Alexa Fluor 594, avidin-rhodamin, and avidin-FITC (all from Invitrogen). All immunostaining experiments were repeated at least three times.

Recombinant fusion proteins

Recombinant fusion proteins NogoΔ20-T7 and NogoΔ21-T7 were purified as described previously (Oertle et al., 2003). In brief, *Escherichia coli* BL21/DE3 were transformed with the bacterial expression vectors pET28 and grown in 2× YT medium (Invitrogen). Expression of the fusion proteins was induced by addition of 1 mM isopropyl-1-thio-β-D-galyctopyranoside (IPTG) to log phase culture at 30°C for 4 h. The highly expressed fusion proteins were purified using the Co^{2+}-Talon Metal Affinity Resin (Takara Bio Inc.). Upon elution with 250 mM imidazole, proteins were extensively dialyzed against PBS, pH 7.4. The purity of the recombinant proteins was confirmed by SDS-PAGE and Coomassie Brilliant blue staining. The protein concentration was determined with a BCA protein assay kit (Thermo Fisher Scientific) using bovine serum albumin as a standard. In addition, an Fc-tagged NogoΔ20 fragment was used (R&D systems).

RhoA pull-down assay and immunostaining

PC12 cells were homogenized in RIPA buffer (50 mM Tris, pH 7.2, 1% Triton X-100, 0.5% sodium deoxycholate, 0.1% SDS, 500 mM NaCl, 10 mM $MgCl_2$, protease inhibitor cocktail [Complete Mini; Roche], and 1 mM PMSF). After centrifugation for 20 min at 13,000 g at 4°C, homogenates (0.5 mg/ml) were incubated for 1 h at 4°C with 60 µg of GST-Rhotekin-RBD beads (Cytoskeleton, Inc.). The beads were then washed twice and eluated in sample buffer. GTP-bound RhoA and total RhoA present in the cell lysates were immunoblotted with 1:200 mouse anti-RhoA antibody (Santa Cruz Biotechnology, Inc.).

Activated Rho was detected by probing cells with the RBD from the Rho-GTP–interacting protein rhotekin-RBD tagged with GST (Cytoskeleton,

Inc.); 20 µg/ml for 1 h at 37°C. 1:400 rabbit anti-GST (Abcam) was used subsequently.

Subcellular fractionation

PC12 cells were cultured on 15-cm plates, serum starved (DME/bovine serum albumin) for 3 h, and either left untreated or treated with NogoΔ20-T7 for 30 min. Next, cells were homogenized in a detergent-free manner with a 22-gauge needle in the homogenization buffer (250 mM sucrose, 3 mM imidazole, 1 mM EDTA, protease inhibitor cocktail [Complete Mini], and 0.03 mM cycloheximide, pH 7.4). Subsequently, a postnuclear supernatant (PNS) was prepared according to standard techniques (Bomsel et al., 1990). The PNS was adjusted to 40.6% sucrose, loaded at the bottom of an SW60 centrifuge tube (Beckman Coulter), and overlaid sequentially with 1.5 volumes of 35% and 1 volume of 25% sucrose solutions in 3 mM imidazole and 1 mM EDTA, pH 7.4. The rest of the tube was filled up with homogenization buffer. The gradient was then centrifuged at 210,000 g at 4°C for 90 min using an SW60 rotor (Beckman Coulter). After centrifugation, different interfaces and sucrose cushions were collected from top to bottom of the tube. The protein concentration of each fraction was determined with BCA protein assay kit using bovine serum albumin as a standard. Equal amounts of protein from each fraction were loaded on SDS-PAGE, followed by immunoblotting with 1:500 mouse anti–EEA-1 (BD), 1:1,000 mouse anti-nucleoporin p62 (BD), 1:5,000 mouse anti-T7 (EMD), and 1:200 mouse anti-RhoA (Santa Cruz Biotechnology, Inc.). This experiment was repeated three times with similar results.

Western blot analysis

Proteins (25–100 µg) were separated by electrophoresis on a 4–12% polyacrylamide gel and transferred to nitrocellulose membranes. Blots were first incubated in a blocking solution of 3% Top Block (VWR International) in TBST (0.1 M Tris base, 0.2% Tween 20, pH 7.4) for 1 h at room temperature, then incubated with primary antibodies overnight at 4°C. After washing with PBS, blots were incubated with a horseradish peroxidase–conjugated anti–rabbit or anti–mouse antibody (Thermo Fisher Scientific) 1:10,000–1:15,000 for 1 h at room temperature. CREB was detected with 1:500 rabbit anti-pCREB (Millipore) and 1:10,000 anti–glyceraldehyde 3-phosphate dehydrogenase (GAPDH; Abcam). Protein bands were detected by adding SuperSignal West Pico Chemiluminescent Substrate (Thermo Fisher Scientific) by exposing the blot in a Stella detector (Raytest). Densitometry analysis was performed with National Institutes of Health software and by normalizing the band intensities to GAPDH values.

Online supplemental material

Fig. S1 shows internalization of NogoΔ20 in the presence of NgR inhibitors. Fig. S2 shows that the retrograde transport of NogoΔ20 is dependent on microtubule and the Pincher protein. Online supplemental material is available at http://www.jcb.org/cgi/content/full/jcb.200906089/DC1.

References

Ahmed, Z., E.L. Suggate, E.R. Brown, R.G. Dent, S.J. Armstrong, L.B. Barrett, M. Berry, and A. Logan. 2006. Schwann cell-derived factor-induced modulation of the NgR/p75NTR/EGFR axis disinhibits axon growth through CNS myelin in vivo and in vitro. *Brain.* 129:1517–1533. doi:10.1093/brain/awl080

Aspenström, P. 1999. Effectors for the Rho GTPases. *Curr. Opin. Cell Biol.* 11:95–102. doi:10.1016/S0955-0674(99)80011-8

Atwal, J.K., J. Pinkston-Gosse, J. Syken, S. Stawicki, Y. Wu, C. Shatz, and M. Tessier-Lavigne. 2008. PirB is a functional receptor for myelin inhibitors of axonal regeneration. *Science.* 322:967–970. doi:10.1126/science.1161151

Bandtlow, C.E., M.F. Schmidt, T.D. Hassinger, M.E. Schwab, and S.B. Kater. 1993. Role of intracellular calcium in NI-35-evoked collapse of neuronal growth cones. *Science.* 259:80–83. doi:10.1126/science.8418499

Bareyre, F.M., B. Haudenschild, and M.E. Schwab. 2002. Long-lasting sprouting and gene expression changes induced by the monoclonal antibody IN-1 in the adult spinal cord. *J. Neurosci.* 22:7097–7110.

Barton, W.A., B.P. Liu, D. Tzvetkova, P.D. Jeffrey, A.E. Fournier, D. Sah, R. Cate, S.M. Strittmatter, and D.B. Nikolov. 2003. Structure and axon outgrowth inhibitor binding of the Nogo-66 receptor and related proteins. *EMBO J.* 22:3291–3302. doi:10.1093/emboj/cdg325

Benmerah, A., C. Lamaze, B. Bègue, S.L. Schmid, A. Dautry-Varsat, and N. Cerf-Bensussan. 1998. AP-2/Eps15 interaction is required for receptor-mediated endocytosis. *J. Cell Biol.* 140:1055–1062. doi:10.1083/jcb.140.5.1055

Bomsel, M., R. Parton, S.A. Kuznetsov, T.A. Schroer, and J. Gruenberg. 1990. Microtubule- and motor-dependent fusion in vitro between apical and basolateral endocytic vesicles from MDCK cells. *Cell.* 62:719–731. doi:10.1016/0092-8674(90)90117-W

Buffo, A., M. Zagrebelsky, A.B. Huber, A. Skerra, M.E. Schwab, P. Strata, and F. Rossi. 2000. Application of neutralizing antibodies against NI-35/250 myelin-associated neurite growth inhibitory proteins to the adult rat cerebellum induces sprouting of uninjured purkinje cell axons. *J. Neurosci.* 20:2275–2286.

Cafferty, W.B., and S.M. Strittmatter. 2006. The Nogo-Nogo receptor pathway limits a spectrum of adult CNS axonal growth. *J. Neurosci.* 26:12242–12250. doi:10.1523/JNEUROSCI.3827-06.2006

Campenot, R.B. 1977. Local control of neurite development by nerve growth factor. *Proc. Natl. Acad. Sci. USA.* 74:4516–4519. doi:10.1073/pnas.74.10.4516

Campenot, R.B., and B.L. MacInnis. 2004. Retrograde transport of neurotrophins: fact and function. *J. Neurobiol.* 58:217–229. doi:10.1002/neu.10322

Caplan, S., N. Naslavsky, L.M. Hartnell, R. Lodge, R.S. Polishchuk, J.G. Donaldson, and J.S. Bonifacino. 2002. A tubular EHD1-containing compartment involved in the recycling of major histocompatibility complex class I molecules to the plasma membrane. *EMBO J.* 21:2557–2567. doi:10.1093/emboj/21.11.2557

Cowan, C.W., Y.R. Shao, M. Sahin, S.M. Shamah, M.Z. Lin, P.L. Greer, S. Gao, E.C. Griffith, J.S. Brugge, and M.E. Greenberg. 2005. Vav family GEFs link activated Ephs to endocytosis and axon guidance. *Neuron.* 46:205–217. doi:10.1016/j.neuron.2005.03.019

Cox, L.J., U. Hengst, N.G. Gurskaya, K.A. Lukyanov, and S.R. Jaffrey. 2008. Intra-axonal translation and retrograde trafficking of CREB promotes neuronal survival. *Nat. Cell Biol.* 10:149–159. doi:10.1038/ncb1677

Daumke, O., R. Lundmark, Y. Vallis, S. Martens, P.J. Butler, and H.T. McMahon. 2007. Architectural and mechanistic insights into an EHD ATPase involved in membrane remodelling. *Nature.* 449:923–927. doi:10.1038/nature06173

Dautry-Varsat, A., A. Ciechanover, and H.F. Lodish. 1983. pH and the recycling of transferrin during receptor-mediated endocytosis. *Proc. Natl. Acad. Sci. USA.* 80:2258–2262. doi:10.1073/pnas.80.8.2258

David, S., and S. Lacroix. 2003. Molecular approaches to spinal cord repair. *Annu. Rev. Neurosci.* 26:411–440. doi:10.1146/annurev.neuro.26.043002.094946

De Camilli, P., K. Takei, and P.S. McPherson. 1995. The function of dynamin in endocytosis. *Curr. Opin. Neurobiol.* 5:559–565. doi:10.1016/0959-4388(95)80059-X

Delcroix, J.D., J.S. Valletta, C. Wu, S.J. Hunt, A.S. Kowal, and W.C. Mobley. 2003. NGF signaling in sensory neurons: evidence that early endosomes carry NGF retrograde signals. *Neuron.* 39:69–84. doi:10.1016/S0896-6273(03)00397-0

Filbin, M.T. 2003. Myelin-associated inhibitors of axonal regeneration in the adult mammalian CNS. *Nat. Rev. Neurosci.* 4:703–713. doi:10.1038/nrn1195

Fish, K.N., S.L. Schmid, and H. Damke. 2000. Evidence that dynamin-2 functions as a signal-transducing GTPase. *J. Cell Biol.* 150:145–154. doi:10.1083/jcb.150.1.145

Fournier, A.E., T. GrandPre, and S.M. Strittmatter. 2001. Identification of a receptor mediating Nogo-66 inhibition of axonal regeneration. *Nature.* 409:341–346. doi:10.1038/35053072

Fournier, A.E., B.T. Takizawa, and S.M. Strittmatter. 2003. Rho kinase inhibition enhances axonal regeneration in the injured CNS. *J. Neurosci.* 23:1416–1423.

Freund, P., E. Schmidlin, T. Wannier, J. Bloch, A. Mir, M.E. Schwab, and E.M. Rouiller. 2006. Nogo-A-specific antibody treatment enhances sprouting and functional recovery after cervical lesion in adult primates. *Nat. Med.* 12:790–792. doi:10.1038/nm1436

Freund, P., E. Schmidlin, T. Wannier, J. Bloch, A. Mir, M.E. Schwab, and E.M. Rouiller. 2009. Anti-Nogo-A antibody treatment promotes recovery of manual dexterity after unilateral cervical lesion in adult primates—re-examination and extension of behavioral data. *Eur. J. Neurosci.* 29:983–996. doi:10.1111/j.1460-9568.2009.06642.x

Galko, M.J., and M. Tessier-Lavigne. 2000. Function of an axonal chemoattractant modulated by metalloprotease activity. *Science.* 289:1365–1367. doi:10.1126/science.289.5483.1365

Gao, Y., K. Deng, J. Hou, J.B. Bryson, A. Barco, E. Nikulina, T. Spencer, W. Mellado, E.R. Kandel, and M.T. Filbin. 2004. Activated CREB is sufficient to overcome inhibitors in myelin and promote spinal axon regeneration in vivo. *Neuron.* 44:609–621. doi:10.1016/j.neuron.2004.10.030

Gianola, S., T. Savio, M.E. Schwab, and F. Rossi. 2003. Cell-autonomous mechanisms and myelin-associated factors contribute to the development of Purkinje axon intracortical plexus in the rat cerebellum. *J. Neurosci.* 23:4613–4624.

Ginty, D.D., and R.A. Segal. 2002. Retrograde neurotrophin signaling: Trk-ing along the axon. *Curr. Opin. Neurobiol.* 12:268–274. doi:10.1016/S0959-4388(02)00326-4

GrandPré, T., F. Nakamura, T. Vartanian, and S.M. Strittmatter. 2000. Identification of the Nogo inhibitor of axon regeneration as a Reticulon protein. *Nature.* 403:439–444. doi:10.1038/35000226

GrandPré, T., S. Li, and S.M. Strittmatter. 2002. Nogo-66 receptor antagonist peptide promotes axonal regeneration. *Nature.* 417:547–551. doi:10.1038/417547a

Grant, B., Y. Zhang, M.C. Paupard, S.X. Lin, D.H. Hall, and D. Hirsh. 2001. Evidence that RME-1, a conserved *C. elegans* EH-domain protein, functions in endocytic recycling. *Nat. Cell Biol.* 3:573–579. doi:10.1038/35078549

Hattori, M., M. Osterfield, and J.G. Flanagan. 2000. Regulated cleavage of a contact-mediated axon repellent. *Science.* 289:1360–1365. doi:10.1126/science.289.5483.1360

He, Z., and M. Tessier-Lavigne. 1997. Neuropilin is a receptor for the axonal chemorepellent Semaphorin III. *Cell.* 90:739–751. doi:10.1016/S0092-8674(00)80534-6

He, X.L., J.F. Bazan, G. McDermott, J.B. Park, K. Wang, M. Tessier-Lavigne, Z. He, and K.C. Garcia. 2003. Structure of the Nogo receptor ectodomain: a recognition module implicated in myelin inhibition. *Neuron.* 38:177–185. doi:10.1016/S0896-6273(03)00232-0

Hopkins, C.R. 1983. Intracellular routing of transferrin and transferrin receptors in epidermoid carcinoma A431 cells. *Cell.* 35:321–330. doi:10.1016/0092-8674(83)90235-0

Howe, C.L., and W.C. Mobley. 2005. Long-distance retrograde neurotrophic signaling. *Curr. Opin. Neurobiol.* 15:40–48. doi:10.1016/j.conb.2005.01.010

Howe, C.L., J.S. Valletta, A.S. Rusnak, and W.C. Mobley. 2001. NGF signaling from clathrin-coated vesicles: evidence that signaling endosomes serve as a platform for the Ras-MAPK pathway. *Neuron.* 32:801–814. doi:10.1016/S0896-6273(01)00526-8

Huang, E.J., and L.F. Reichardt. 2001. Neurotrophins: roles in neuronal development and function. *Annu. Rev. Neurosci.* 24:677–736. doi:10.1146/annurev.neuro.24.1.677

Huber, A.B., O. Weinmann, C. Brösamle, T. Oertle, and M.E. Schwab. 2002. Patterns of Nogo mRNA and protein expression in the developing and adult rat and after CNS lesions. *J. Neurosci.* 22:3553–3567.

Jurewicz, A., M. Matysiak, C.S. Raine, and K. Selmaj. 2007. Soluble Nogo-A, an inhibitor of axonal regeneration, as a biomarker for multiple sclerosis. *Neurology.* 68:283–287. doi:10.1212/01.wnl.0000252357.30287.1d

Kaech, S., and G. Banker. 2006. Culturing hippocampal neurons. *Nat. Protoc.* 1:2406–2415. doi:10.1038/nprot.2006.356

Kapfhammer, J.P., H. Xu, and J.A. Raper. 2007. The detection and quantification of growth cone collapsing activities. *Nat. Protoc.* 2:2005–2011. doi:10.1038/nprot.2007.295

Kim, J.E., B.P. Liu, J.H. Park, and S.M. Strittmatter. 2004. Nogo-66 receptor prevents raphespinal and rubrospinal axon regeneration and limits functional recovery from spinal cord injury. *Neuron.* 44:439–451. doi:10.1016/j.neuron.2004.10.015

Kirkham, M., A. Fujita, R. Chadda, S.J. Nixon, T.V. Kurzchalia, D.K. Sharma, R.E. Pagano, J.F. Hancock, S. Mayor, and R.G. Parton. 2005. Ultrastructural identification of uncoated caveolin-independent early endocytic vehicles. *J. Cell Biol.* 168:465–476. doi:10.1083/jcb.200407078

Kolodkin, A.L., D.V. Levengood, E.G. Rowe, Y.T. Tai, R.J. Giger, and D.D. Ginty. 1997. Neuropilin is a semaphorin III receptor. *Cell.* 90:753–762. doi:10.1016/S0092-8674(00)80535-8

Kreutzberg, G.W. 1969. Neuronal dynamics and axonal flow. IV. Blockage of intra-axonal enzyme transport by colchicine. *Proc. Natl. Acad. Sci. USA.* 62:722–728. doi:10.1073/pnas.62.3.722

Le Roy, C., and J.L. Wrana. 2005. Clathrin- and non-clathrin-mediated endocytic regulation of cell signalling. *Nat. Rev. Mol. Cell Biol.* 6:112–126. doi:10.1038/nrm1571

Liebscher, T., L. Schnell, D. Schnell, J. Scholl, R. Schneider, M. Gullo, K. Fouad, A. Mir, M. Rausch, D. Kindler, et al. 2005. Nogo-A antibody improves regeneration and locomotion of spinal cord-injured rats. *Ann. Neurol.* 58:706–719. doi:10.1002/ana.20627

Luo, Y., D. Raible, and J.A. Raper. 1993. Collapsin: a protein in brain that induces the collapse and paralysis of neuronal growth cones. *Cell.* 75:217–227. doi:10.1016/0092-8674(93)80064-L

Marston, D.J., S. Dickinson, and C.D. Nobes. 2003. Rac-dependent transendocytosis of ephrinBs regulates Eph-ephrin contact repulsion. *Nat. Cell Biol.* 5:879–888. doi:10.1038/ncb1044

Mayor, S., and R.E. Pagano. 2007. Pathways of clathrin-independent endocytosis. *Nat. Rev. Mol. Cell Biol.* 8:603–612. doi:10.1038/nrm2216

McGee, A.W., Y. Yang, Q.S. Fischer, N.W. Daw, and S.M. Strittmatter. 2005. Experience-driven plasticity of visual cortex limited by myelin and Nogo receptor. *Science.* 309:2222–2226. doi:10.1126/science.1114362

Mi, S., X. Lee, Z. Shao, G. Thill, B. Ji, J. Relton, M. Levesque, N. Allaire, S. Perrin, B. Sands, et al. 2004. LINGO-1 is a component of the Nogo-66 receptor/p75 signaling complex. *Nat. Neurosci.* 7:221–228. doi:10.1038/nn1188

Monard, D. 1988. Cell-derived proteases and protease inhibitors as regulators of neurite outgrowth. *Trends Neurosci.* 11:541–544. doi:10.1016/0166-2236(88)90182-8

Montani, L., B. Gerrits, P. Gehrig, A. Kempf, L. Dimou, B. Wollscheid, and M.E. Schwab. 2009. Neuronal Nogo-A modulates growth cone motility via Rho-GTP/LIMK1/cofilin in the unlesioned adult nervous system. *J. Biol. Chem.* 284:10793–10807. doi:10.1074/jbc.M808297200

Mu, F.T., J.M. Callaghan, O. Steele-Mortimer, H. Stenmark, R.G. Parton, P.L. Campbell, J. McCluskey, J.P. Yeo, E.P. Tock, and B.H. Toh. 1995. EEA1, an early endosome-associated protein. EEA1 is a conserved alpha-helical peripheral membrane protein flanked by cysteine "fingers" and contains a calmodulin-binding IQ motif. *J. Biol. Chem.* 270:13503–13511. doi:10.1074/jbc.270.22.13503

Niederöst, B.P., D.R. Zimmermann, M.E. Schwab, and C.E. Bandtlow. 1999. Bovine CNS myelin contains neurite growth-inhibitory activity associated with chondroitin sulfate proteoglycans. *J. Neurosci.* 19:8979–8989.

Niederöst, B., T. Oertle, J. Fritsche, R.A. McKinney, and C.E. Bandtlow. 2002. Nogo-A and myelin-associated glycoprotein mediate neurite growth inhibition by antagonistic regulation of RhoA and Rac1. *J. Neurosci.* 22:10368–10376.

Oertle, T., M.E. van der Haar, C.E. Bandtlow, A. Robeva, P. Burfeind, A. Buss, A.B. Huber, M. Simonen, L. Schnell, C. Brösamle, et al. 2003. Nogo-A inhibits neurite outgrowth and cell spreading with three discrete regions. *J. Neurosci.* 23:5393–5406.

Oh, P., D.P. McIntosh, and J.E. Schnitzer. 1998. Dynamin at the neck of caveolae mediates their budding to form transport vesicles by GTP-driven fission from the plasma membrane of endothelium. *J. Cell Biol.* 141:101–114. doi:10.1083/jcb.141.1.101

Pelkmans, L., D. Püntener, and A. Helenius. 2002. Local actin polymerization and dynamin recruitment in SV40-induced internalization of caveolae. *Science.* 296:535–539. doi:10.1126/science.1069784

Prinjha, R., S.E. Moore, M. Vinson, S. Blake, R. Morrow, G. Christie, D. Michalovich, D.L. Simmons, and F.S. Walsh. 2000. Inhibitor of neurite outgrowth in humans. *Nature.* 403:383–384. doi:10.1038/35000287

Ren, X.D., W.B. Kiosses, and M.A. Schwartz. 1999. Regulation of the small GTP-binding protein Rho by cell adhesion and the cytoskeleton. *EMBO J.* 18:578–585. doi:10.1093/emboj/18.3.578

Riccio, A., B.A. Pierchala, C.L. Ciarallo, and D.D. Ginty. 1997. An NGF-TrkA-mediated retrograde signal to transcription factor CREB in sympathetic neurons. *Science.* 277:1097–1100. doi:10.1126/science.277.5329.1097

Schwab, M.E. 2004. Nogo and axon regeneration. *Curr. Opin. Neurobiol.* 14:118–124. doi:10.1016/j.conb.2004.01.004

Shao, Y., W. Akmentin, J.J. Toledo-Aral, J. Rosenbaum, G. Valdez, J.B. Cabot, B.S. Hilbush, and S. Halegoua. 2002. Pincher, a pinocytic chaperone for nerve growth factor/TrkA signaling endosomes. *J. Cell Biol.* 157:679–691. doi:10.1083/jcb.200201063

Tamagnone, L., S. Artigiani, H. Chen, Z. He, G.I. Ming, H. Song, A. Chedotal, M.L. Winberg, C.S. Goodman, M. Poo, et al. 1999. Plexins are a large family of receptors for transmembrane, secreted, and GPI-anchored semaphorins in vertebrates. *Cell.* 99:71–80. doi:10.1016/S0092-8674(00)80063-X

Valdez, G., W. Akmentin, P. Philippidou, R. Kuruvilla, D.D. Ginty, and S. Halegoua. 2005. Pincher-mediated macroendocytosis underlies retrograde signaling by neurotrophin receptors. *J. Neurosci.* 25:5236–5247. doi:10.1523/JNEUROSCI.5104-04.2005

Valdez, G., P. Philippidou, J. Rosenbaum, W. Akmentin, Y. Shao, and S. Halegoua. 2007. Trk-signaling endosomes are generated by Rac-dependent macro-endocytosis. *Proc. Natl. Acad. Sci. USA.* 104:12270–12275. doi:10.1073/pnas.0702819104

Wang, X., S.J. Chun, H. Treloar, T. Vartanian, C.A. Greer, and S.M. Strittmatter. 2002. Localization of Nogo-A and Nogo-66 receptor proteins at sites of axon-myelin and synaptic contact. *J. Neurosci.* 22:5505–5515.

Watson, F.L., H.M. Heerssen, D.B. Moheban, M.Z. Lin, C.M. Sauvageot, A. Bhattacharyya, S.L. Pomeroy, and R.A. Segal. 1999. Rapid nuclear responses to target-derived neurotrophins require retrograde transport of ligand-receptor complex. *J. Neurosci.* 19:7889–7900.

Wong, S.T., J.R. Henley, K.C. Kanning, K.H. Huang, M. Bothwell, and M.M. Poo. 2002. A p75(NTR) and Nogo receptor complex mediates repulsive signaling by myelin-associated glycoprotein. *Nat. Neurosci.* 5:1302–1308. doi:10.1038/nn975

Wu, C., B. Cui, L. He, L. Chen, and W.C. Mobley. 2009. The coming of age of axonal neurotrophin signaling endosomes. *J. Proteomics.* 72:46–55. doi:10.1016/j.jprot.2008.10.007

Yiu, G., and Z. He. 2003. Signaling mechanisms of the myelin inhibitors of axon regeneration. *Curr. Opin. Neurobiol.* 13:545–551. doi:10.1016/j.conb.2003.09.006

Yiu, G., and Z. He. 2006. Glial inhibition of CNS axon regeneration. *Nat. Rev. Neurosci.* 7:617–627. doi:10.1038/nrn1956

Zimmer, M., A. Palmer, J. Köhler, and R. Klein. 2003. EphB-ephrinB bi-directional endocytosis terminates adhesion allowing contact mediated repulsion. *Nat. Cell Biol.* 5:869–878. doi:10.1038/ncb1045